Probing the potential and reaction coupling effects of ^{6,7}Li + ^{28}Si at sub- and near-barrier energies with elastic backscattering

K. Zerva,[1] A. Pakou,[1,*] K. Rusek,[2,3] N. Patronis,[1] N. Alamanos,[4] X. Aslanoglou,[1] D. Filipescu,[5] T. Glodariu,[5] N. Keeley,[3] M. Kokkoris,[6] M. La Commara,[7] A. Lagoyannis,[8] M. Mazzocco,[9] N. G. Nicolis,[1] D. Pierroutsakou,[10] and M. Romoli[10]

[1]*Department of Physics and HINP, The University of Ioannina, GR-45110 Ioannina, Greece*
[2]*Heavy Ion Laboratory, University of Warsaw, Warsaw, Poland*
[3]*Department of Nuclear Reactions, Andrzej Sołtan Institute for Nuclear Studies, Warsaw, Poland*
[4]*CEA-Saclay DSM/IRFU/DIR, F-91191 Gif-sur-Yvette, France*
[5]*"Horia Hulubei" National Institute of Physics and Nuclear Engineering, Romania*
[6]*National Technical University of Athens, Greece*
[7]*Dipartimento di Scienze Fisiche and INFN Sezione di Napoli, I-80125, Napoli, Italy*
[8]*National Research Center Demokritos, Greece*
[9]*Dipartimento di Fisica, INFN, I-35131 Padova, Italy*
[10]*INFN Sezione di Napoli, I-80125, Napoli, Italy*

(Received 17 May 2010; revised manuscript received 11 August 2010; published 11 October 2010)

The excitation functions for ^{7}Li + ^{28}Si quasielastic scattering at 150° and 170° have been measured at sub- and near-barrier energies (0.6 to 1.3 V_B) and the corresponding barrier distributions derived. The results were analyzed within the framework of the optical model using a procedure similar to one used on previous results for ^{6}Li + ^{28}Si employing double-folded potentials calculated using the BDM3Y1 effective interaction. The variation of the surface strength of the optical potential as a function of incident energy was compared for the two systems ^{6}Li + ^{28}Si and ^{7}Li + ^{28}Si, the barrier distributions being used to help better define the potential at the lowest energies. The barrier distributions were also analyzed with continuum-discretized coupled-channel (CDCC) and coupled reaction channel (CRC) calculations as a means of investigating the influence of breakup and transfer reactions on these quantities for these light, weakly bound projectiles.

DOI: 10.1103/PhysRevC.82.044607 PACS number(s): 25.70.Bc, 24.10.Ht, 24.50.+g

I. INTRODUCTION

The contribution of coupling effects to near-barrier fusion cross sections and elastic scattering has been extensively investigated in the past [1–4]. To describe the elastic scattering, either these couplings have to be taken into account explicitly through coupled-channel theories, or the various optical model parameters must be allowed to vary substantially with incident energy as the Coulomb barrier is approached (the "threshold anomaly").

The influence of couplings on near-barrier fusion cross sections was further elucidated by barrier distributions extracted from precise fusion excitation function measurements, a method initially suggested by Rowley, Satchler, and Stelson [5]. Similar results were obtained with backward-angle quasielastic [6] and elastic [7] scattering excitation functions forming barrier distributions via their first derivatives:

$$D_{\rm qel}(E) = -\frac{d}{dE}\left[\frac{d\sigma_{\rm qel}}{d\sigma_{\rm Ruth}}(E)\right], \qquad (1)$$

$$D_{\rm el}(E) = -\frac{d}{dE}\left[\sqrt{\frac{d\sigma_{\rm el}}{d\sigma_{\rm Ruth}}(E)}\right].$$

The role of backscattering measurements in probing the properties of the optical potential has also been important in recent years. A large amount of work has been devoted to systematic studies of the surface properties of the optical model potential (diffusivity of Woods-Saxon potentials) through high-precision backward-angle quasielastic scattering measurements [8–13] at sub-barrier energies. At these backward angles, deviations from unity of the ratio to Rutherford of the (quasi)elastic cross sections are mainly sensitive to the surface properties of the potential [9].

Recently, going a step further, we used the elastic backscattering as a tool to help probe the energy dependence of the potential at near- and sub-barrier energies for the weakly bound nucleus ^{6}Li scattered by the light target ^{28}Si [14]. Previous inconsistencies [15,16] with regard to the new potential anomaly observed in this system were clarified. Additionally, continuum-discretized coupled-channel (CDCC) calculations for the ^{6}Li $\rightarrow \alpha + d$ breakup were performed to investigate the influence of this coupling on the barrier distribution, but no transfer coupling was included.

By extending our backscattering measurements to ^{7}Li + ^{28}Si, in this work we compare the two systems, ^{6}Li + ^{28}Si and ^{7}Li + ^{28}Si, in order to investigate differences in the behavior of the optical model potential for these two weakly bound projectiles. CDCC calculations are presented for the ^{7}Li + ^{28}Si system and coupled reaction channel (CRC) calculations for the ^{6}Li + ^{28}Si system, where couplings to the (^{6}Li,^{5}Li) single-neutron stripping channels were added to the ^{6}Li breakup couplings included in the CDCC calculations of our previous work [14]. In this work we shall refer to calculations that include breakup couplings alone as CDCC,

*Corresponding author: apakou@cc.uoi.gr

while calculations that include both breakup and transfer couplings will be referred to as CRC. All CDCC and CRC calculations presented in this work were performed using the code FRESCO [17].

A few other measurements of the elastic and quasielastic backscattering for weakly bound nuclei have been reported previously [18–22], but they were for heavier targets and emphasized the coupling effects rather than the energy dependence of the optical potential.

II. EXPERIMENTAL DETAILS AND DATA REDUCTION

Details of the experimental method were given in [14]. We give here some points pertinent to this work. Beams of $^{6,7}Li^{3+}$ ions were delivered by the TN11/25 HVEC 5.5 MV Tandem accelerator of the National Research Center of Greece-Demokritos at several bombarding energies from 5 to 12 MeV. Beam currents were of the order of 1–5 nA. The beams impinged on a 200 $\mu g/cm^2$ thick self-supporting ^{28}Si target, with the target frame fixed perpendicular to the beam direction. (Quasi)elastic backscattering events were recorded in four silicon detectors set at $\pm 150^\circ$ and $\pm 170^\circ$ (for ^{7}Li, quasielastic events were recorded because the ^{7}Li $1/2^-$ first excited state could not be separated). The beam flux was normalized via a measurement of the Rutherford scattering in two silicon detectors set at $\pm 30^\circ$.

Ratios of the (quasi)elastic cross sections to Rutherford were formed as follows:

$$\frac{\sigma_{el}}{\sigma_{Ruth}}(170^\circ\text{–}150^\circ) = \frac{N(170^\circ\text{–}150^\circ)}{N(30^\circ)} \frac{\sigma_{Ruth}(30)}{\sigma_{Ruth}(170)} \frac{\Omega_{30}}{\Omega_{170(150)}}, \quad (2)$$

where N_{30} and $N_{170(150)}$ are the (quasi)elastic scattering total counts in the forward and backward detectors, and Ω_{30} and $\Omega_{170(150)}$ are their respective solid angles. The ratio of solid angles was determined during the experiment by scattering 11 MeV lithium ions from a thin gold target. At this energy, the elastic scattering is pure Rutherford for both forward and backward detectors, and the ratio of solid angles can be determined with negligible error. Therefore, the only errors involved in relation (2) are the statistical errors, which at most of the energies were less than 2%, except at the highest energies where they were up to 20%, partly due to the low beam current available from the accelerator in combination with the small backward-angle elastic cross section at these energies and partly due to a high background. This background was partly due to scattering and partly to reaction products giving a continuous energy spectrum. In future measurements, this "background" could be avoided with the use of telescopes with gas detectors in the first stage, since the energy of the recoiling lithium is very small.

III. EXCITATION FUNCTIONS AND BARRIER DISTRIBUTIONS: OPTICAL MODEL ANALYSIS

The excitation function for $^7Li + ^{28}Si$ is shown in Fig. 1(a) while the corresponding barrier distribution, obtained using the left-hand relation of equation (1), is shown in Fig. 1(b). Previous results for $^6Li + ^{28}Si$ [14] are repeated in Figs. 2(a) and 2(b) for ease of comparison. As noted above, for ^{7}Li the 0.478 MeV $1/2^-$ inelastic peak was not resolved, and the results are quasielastic rather than elastic scattering. However, we consider that the quasielastic nature of the ^{7}Li data is not an impediment to our comparisons with the ^{6}Li elastic scattering data or in general for our conclusions. According to the two-channel calculations described in Sec. IV, the influence of the inelastic scattering on the barrier distribution is negligible. This is demonstrated in Fig. 3, where two calculated barrier distributions for $^7Li + ^{28}Si$ two-channel calculations (including reorientation of the ^{7}Li ground state and excitation to its first excited state only) are presented, one for the pure elastic scattering and one for the quasielastic scattering including excitation of the experimentally unresolved ^{7}Li $1/2^-$ first excited state. The resulting barrier distributions are essentially identical.

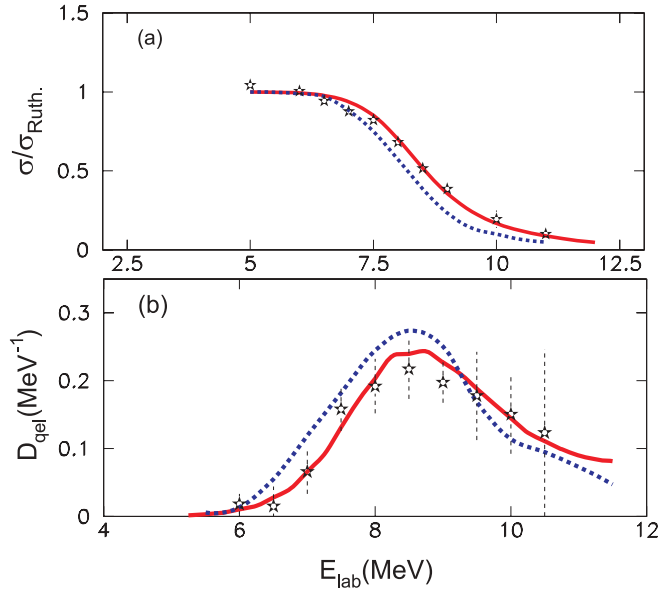

FIG. 1. (Color online) (a) Quasielastic cross sections (stars), the error-weighted mean of the measured cross sections at 150° and 170°, as a function of laboratory energy for $^7Li + ^{28}Si$. The associated errors do not exceed the size of the data points and in most cases are of the order of 2%, although at the highest energies they are up to 20%. The lines represent ECIS calculations with the optical potentials presented in Fig. 4, with the same notation. The dashed line represents calculations using an optical potential where the real and imaginary parts obey a dispersion relation, while the solid line represents calculations where they do not (see text). (b) Barrier distributions derived from the excitation functions shown in (a).

The interpretation of the backscattering results within the optical model framework is described in the following subsection.

A. $^7Li + ^{28}Si$

In Fig. 4, we present previous results on the potential anomaly, obtained within the double-folding model framework [16] using the BDM3Y1 effective interaction. The decreasing trend of the imaginary potential strength approaching the barrier is readily apparent. First, adopting such a behavior for

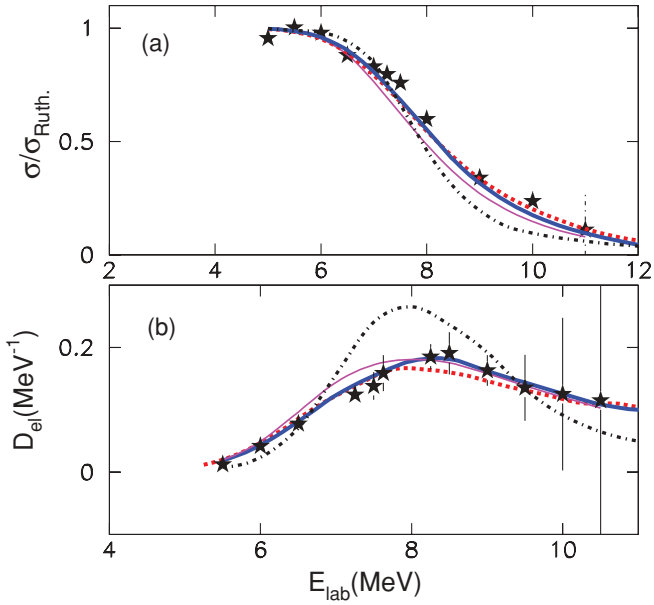

FIG. 2. (Color online) (a) Previously measured elastic scattering cross sections [14], the error-weighted mean of the measured cross sections at 150° and 170°, as a function of laboratory energy for ^{6}Li + ^{28}Si. The lines represent ECIS calculations with the optical potentials presented in Fig. 5, with the same notation. The dot-dashed line (black) corresponds to a decreasing imaginary potential from higher to lower energies, the solid line (blue) corresponds to an increasing imaginary potential, which best fits the backscattering data. The thin solid line (pink) represents a similar imaginary potential but which drops to zero earlier, and finally the dashed line (red) represents a potential with an increasing trend from above but with a steeper slope. (b) Elastic backscattering barrier distributions with the same notation as in (a).

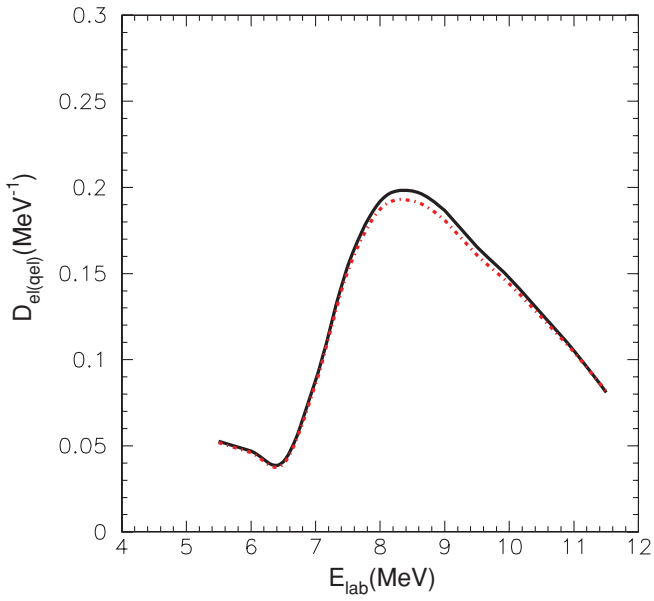

FIG. 3. (Color online) Barrier distributions for ^{7}Li + ^{28}Si calculated for elastic scattering (solid line) and for quasielastic scattering (dot-dashed line) calculated with a two-channel model taking into account reorientation of the ^{7}Li ground state and excitation to the first excited state.

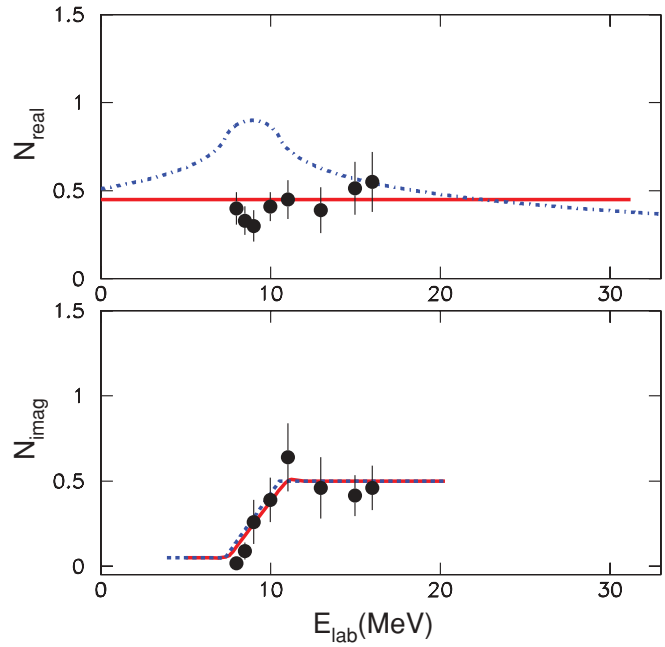

FIG. 4. (Color online) Previously determined normalization factors of the ^{7}Li + ^{28}Si real and imaginary potential as a function of ^{7}Li bombarding energy [16], denoted by the solid circles. To describe the behavior of the imaginary potential we draw two lines, one constant and one decreasing with decreasing energy. At low energies, a "step" of 0.1 MeV is additionally considered. Two corresponding real potentials are given: the dot-dashed curve represents a potential derived from the imaginary part via the dispersion relation [23] and the solid line is an energy-independent curve drawn through the empirical points without taking the dispersion relation into account.

the imaginary part, we calculated the expected energy variation of the real part of the potential with the dispersion relation [23], designated in the figure by the bell-shaped dot-dashed curve. Second, assuming that the dispersion relation does not hold for the ^{7}Li + ^{28}Si system, we simply drew a straight line through the points denoting the strength of the real part of the potential, i.e., no variation with energy. With these two potentials—the bell-shaped and constant real parts with in both cases the same imaginary part—we calculated the corresponding backward-angle elastic scattering cross sections as a function of energy. The results are shown in Figs. 1(a) and 1(b) for the excitation function and the corresponding barrier distribution, respectively. It is obvious that the appropriate optical potential is that where the real part is described by a straight line and which therefore does not obey the dispersion relation. We note that the "step" in the imaginary potential at very low energies, equal to a constant surface imaginary potential strength of 0.1 MeV, is necessary in order to fit the barrier distribution. A constant imaginary potential at sub-barrier energies implies a continuous loss of flux to reaction channels other than elastic scattering, possibly to transfer. Experimental evidence for a strong transfer channel at low energies with a transfer-to-total cross section ratio that increases with decreasing energy below the barrier is given in Ref. [24]. Moreover, we note that some evidence for similar behavior of the imaginary potential in the ^{7}Li + ^{208}Pb system was found by Keeley *et al.* [25] and

attributed to a continuous loss of flux, suggested as possibly being due to Coulomb breakup, impossible for the present case because of the low atomic number of the target. We also note the unusual behavior presented in a recent elastic scattering study of the ^{7}Li + ^{144}Sm system [26], where the imaginary part remains constant till very low energies well below the Coulomb barrier, while the real part shows a slight increasing behavior. It therefore appears that the type of potential anomaly for ^{7}Li is not always consistent with the traditional type met with for tightly bound projectiles, while it is strongly dependent on the target and therefore on the open reaction channels in this low-energy regime.

B. ^{6}Li + ^{28}Si

In Fig. 5, we present previous results on the potential anomaly obtained from optical model fits to angular distribution measurements within the double-folding framework [15] using the BDM3Y1 effective interaction. In the same figure, we also present results from Ref. [14] where using a similar procedure we had attempted to define in a more accurate way the optical potential, extending its energy dependence to lower energies. The results of the analysis of the elastic backscattering according to the various alternative optical potentials described in detail in Ref. [14] are presented in Figs. 2(a) and 2(b) for the excitation function and barrier distribution, respectively. It is apparent that the potential which best reproduces all the data is that with an imaginary part having a small but definite increasing trend as the incident energy is lowered toward the Coulomb barrier, see Fig. 5, and which extends to very low energies before dropping to zero.

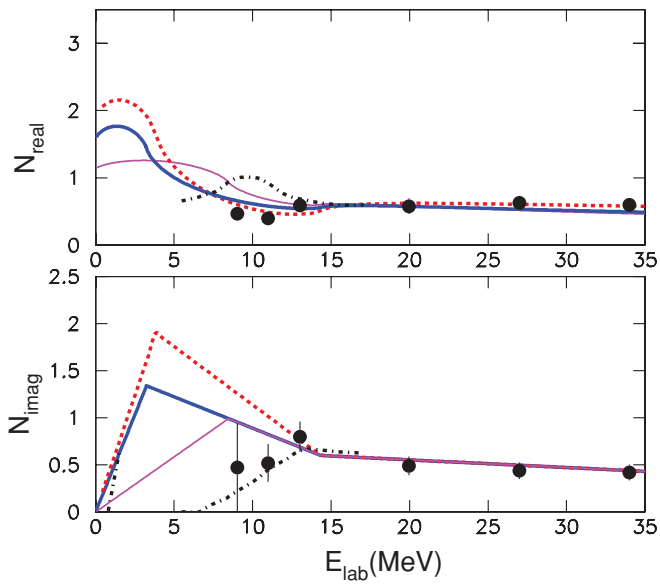

FIG. 5. (Color online) Previously determined normalization factors of the ^{6}Li + ^{28}Si real and imaginary potentials as a function of the ^{6}Li bombarding energy [15], denoted by the solid circles. For the imaginary potential we have made four different assumptions (dot-dashed black, dashed red, solid blue, and thin solid pink lines). The corresponding real potentials were calculated using the dispersion relation [23].

It is also obvious by comparing Figs. 4 and 5 that the fall of the imaginary potential starts much later (i.e. ,at lower energies) for ^{6}Li than for ^{7}Li. In more detail, while for ^{6}Li the imaginary potential around the barrier starts to increase and then at very low energies drops to zero, for ^{7}Li its starts to drop around the barrier but does not continue to zero, rather presenting a flat behavior to very low energies. The above analysis made it clear that the elastic scattering barrier distribution can be a valuable tool for mapping the threshold anomaly. Moreover, it can be used to help further extend below the barrier the energy dependence of the optical potential.

IV. REACTION MECHANISMS

A. Effects of breakup

In our previous work [14], we showed by means of CDCC calculations that the breakup of ^{6}Li strongly affects the barrier distribution for the ^{6}Li + ^{28}Si system, shifting it to slightly higher energies and reducing the peak height by at least 20% while simultaneously making the distribution more broad.

In this work, we have performed similar calculations for ^{7}Li + ^{28}Si, following closely those presented in Ref. [16]. It was assumed that ^{7}Li has a two-body $\alpha + t$ cluster structure. Couplings between bound states of ^{7}Li (the ground and first excited state) as well as resonant and nonresonant cluster states from the continuum were included, with multipolarity up to $\Delta L = 3$. The continuum above the breakup threshold was discretized into momentum bins of width $\Delta k = 0.25$ fm^{-1}. In the presence of resonances (the $7/2^{-}$ at $E_x = 4.63$ MeV and the $5/2^{-}$ at 6.68 MeV), this binning scheme was modified to avoid double counting. The continuum was truncated at about 12 MeV excitation energy at the highest beam energy. This was reduced at lower beam energies according to the appropriate value of the center-of-mass energy of the scattering system. All diagonal and coupling potentials were generated from empirical α + target and t + target optical model potentials using single folding. The calculations reproduced well the data for ^{7}Li + ^{28}Si elastic scattering [16] over the beam energy range 8–16 MeV with one free parameter: renormalization of the real parts of the input potentials, set to $N_r = 0.6$.

Since in the backscattering measurements the inelastic part was not resolved from the elastic part, the calculations for ^{7}Li represent the quasielastic scattering (elastic + excitation of ^{7}Li to its first excited state). The backscattering results are presented in Fig. 6(a). The dot-dashed curve shows the results of two-channel calculations, with just reorientation of the ^{7}Li ground state and excitation to the first excited state included. The results of the full CDCC calculations with couplings to the resonant and nonresonant states of the $\alpha + t$ continuum included are plotted as the solid curve. The effect of breakup channels on the barrier distribution is very small, much smaller than for ^{6}Li + ^{28}Si (the results for this system taken from Ref. [14] are given in Fig. 6(b) for ease of reference). This may be due to the almost negligible breakup cross section for ^{7}Li compared to that for ^{6}Li.

B. Effects of transfer reactions

In a series of experiments aimed at studying the ^{6}Li + ^{28}Si interaction [16,24,27,28], it was found that the largest cross

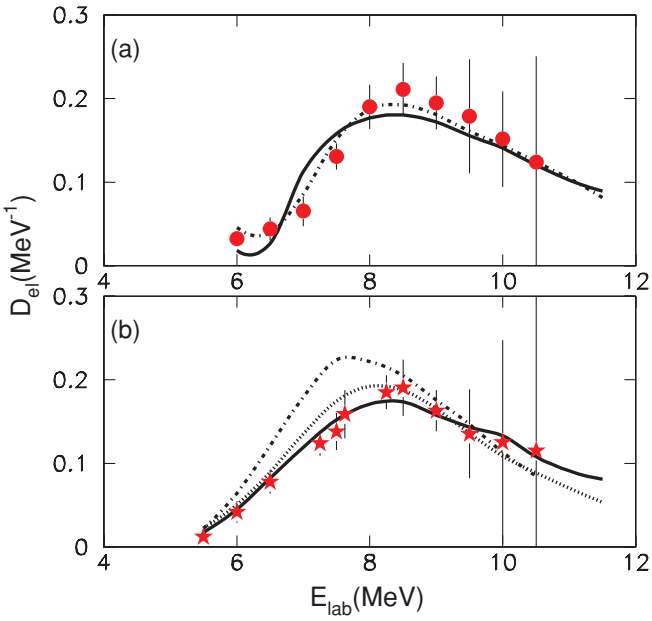

FIG. 6. (Color online) Coupling effects on the elastic backscattering barrier distributions: (a) ^{7}Li + ^{28}Si data (solid circles) and (b) ^{6}Li + ^{28}Si data (solid stars). The dot-dashed curves show the results of optical model calculations with the bare potentials, while the solid curves denote calculations including the $^{7}\text{Li} \rightarrow \alpha + t$ and $^{6}\text{Li} \rightarrow \alpha + d$ breakup for (a) and (b), respectively. For ^{6}Li + ^{28}Si the 1n-transfer reaction ^{28}Si(^{6}Li,^{5}Li)^{29}Si was taken into account, and the dotted curve represents the results of CRC calculations with the breakup and transfer couplings included simultaneously.

section is for one-neutron transfer leading to excited states in ^{29}Si at excitation energies above 1.27 MeV. The value of the summed cross section for this reaction at an incident energy of 13 MeV was 113±29 mb, more than five times larger than that for $^{6}\text{Li} \rightarrow \alpha + d$ breakup. We therefore investigated how much this process affects the elastic scattering and thus the barrier distribution.

We performed CRC calculations with couplings to breakup and one-neutron transfer channels explicitly included, as indicated in Fig. 7. In these calculations we assumed that the transfer reaction may lead to ^{5}Li in its ground and first excited states (both are resonant states in the α+p continuum) and that the final nucleus, ^{29}Si, could be excited to states up to 6.5 MeV. Eight states of ^{29}Si in this energy range, with the largest spectroscopic amplitudes, were taken into account. Details of CDCC

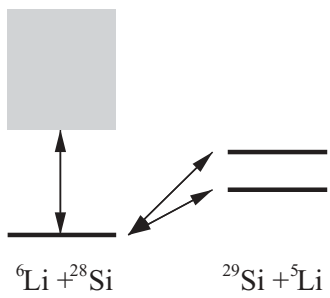

FIG. 7. Coupling scheme used in the ^{6}Li + ^{28}Si CRC calculations.

calculations for $^{6}\text{Li} \rightarrow \alpha + d$ breakup as well as distorted-wave Born approximation (DWBA) calculations for one-neutron transfer may be found in Refs. [16,27,29]. The calculations reproduced the experimental data for ^{6}Li breakup [27]. However, they underestimated the measured one-neutron transfer cross section. To improve the latter agreement, the spectroscopic amplitudes had to be renormalized by a factor of 2.

The effect of breakup and one-neutron transfer on the ^{6}Li elastic backscattering is illustrated in Fig. 6(b). Inclusion of the $^{6}\text{Li} \rightarrow \alpha + d$ breakup coupling significantly affects the barrier distribution, reducing the maximum height by at least 20%. The effect of one-neutron transfer is much smaller, even with the renormalized spectroscopic amplitudes. These results demonstrate that transfer and breakup have opposite effects in this case and that the coupling effect is not proportional to the cross section of a particular process but rather depends on its nature.

We have not attempted CRC calculations for the ^{7}Li system, as here the most important transfer partition is the ^{28}Si(^{7}Li,^{5}Li)^{30}Si two-neutron stripping reaction [24], and the corresponding calculations are more technically challenging. Due to the light target, two-step paths may contribute significantly to the reaction mechanism. Test calculations in which only the single-step direct transfer of a dineutron-like cluster was considered gave unrealistically large coupling effects, completely destroying the agreement with the measured barrier distribution obtained with the two-channel and full CDCC calculations while considerably underestimating the measured transfer cross section. More sophisticated calculations including two-step transfer paths proceeding via the (^{7}Li,^{6}Li) one-neutron transfer are left for the future, since the currently available data are not accurate enough to trace the expected small differences in the barrier distributions between full CRC calculations and simple two-channel calculations because the latter reproduce adequately well these data.

V. SUMMARY AND CONCLUSIONS

Elastic backscattering measurements were performed for the ^{7}Li + ^{28}Si system at sub- and near-barrier energies and the barrier distribution was derived. The results were presented together with previous ones on ^{6}Li + ^{28}Si for purposes of comparison.

It was found that elastic backscattering can be a useful tool to probe the optical model potential at sub-barrier energies. For ^{6}Li + ^{28}Si, it was found that an imaginary potential that increases in surface strength as the incident energy is reduced toward the Coulomb barrier best reproduces the whole data set, as is the case for all other systems involving this weakly bound projectile. The resulting potential behavior is consistent with the dispersion relation and gives a real part almost independent of energy with a small dip around the barrier, with a bell-shaped peak appearing at very low energies, the latter being essentially impossible to confirm experimentally. However, the technique of combining angular distribution measurements with their rather low sensitivity to the potential at near-barrier energies with measurements of the (quasi)elastic barrier distribution appears a promising way to extend our knowledge of the potential to sub-barrier energies.

On the other hand, for ^{7}Li + ^{28}Si, it was found that, in contrast to ^{6}Li, the imaginary part of the optical potential reduces as we approach the barrier at much higher energies following the well-established behavior for tightly bound nuclei, but does not seem to continue to zero below the barrier. Rather, there is evidence of a continuous loss of flux at deep sub-barrier energies in the shape of a flat, nonzero imaginary potential in this energy regime, possibly due to positive Q-value transfer channels in this case. This imaginary potential is not connected via a dispersion relation with the real one, the latter presenting a rather constant behavior as a function of energy to very low energies.

(Quasi)elastic backscattering barrier distributions are also a good means of probing coupling effects at near-barrier energies. While breakup cross sections with this low Z target are very small, coupling to the continuum has a strong influence on the elastic channel for ^{6}Li. On the other hand, transfer presents a large cross section but has a small coupling influence, of opposite sign to that for breakup. For ^{7}Li, it was found that the barrier distribution could be well described by two-channel calculations including just ground-state reorientation and coupling to the ^{7}Li $1/2^{-}$ first excited state, suggesting that other couplings should have a negligible influence.

ACKNOWLEDGMENTS

One of us (K. Zerva) warmly acknowledges a three years financial support in the context of a research Project co-funded by the European Union - European Social Fund (ESF) & National Sources, in the framework of the program "HRAKLEITOS II" of the "Operational Program Education and Life Long Learning" of the Hellenic Ministry of Education, Lifelong Learning and Religion. We would also like to warmly acknowledge Massimo Loriggiola (Laboratori Nazionali di Legnaro, Italy) for providing the silicon targets.

[1] M. Dasgupta, D. Hinde, N. Rowley, and A. Stefanini, Annu. Rev. Nucl. Part. Sci. **48**, 401 (1998).
[2] L. F. Canto, P. R. S. Gomes, R. Donangelo, and M. S. Hussein, Phys. Rep. **424**, 1 (2006).
[3] N. Keeley, R. Raabe, N. Alamanos, and J. L. Sida, Prog. Part. Nucl. Phys. **59**, 579 (2007).
[4] N. Keeley, N. Alamanos, K. W. Kemper, and K. Rusek, Prog. Part. Nucl. Phys. **63**, 396 (2009).
[5] N. Rowley, G. R. Satchler, and P. H. Stelson, Phys. Lett. B **254**, 25 (1991).
[6] H. Timmers *et al.*, Nucl. Phys. A **584**, 190 (1995).
[7] N. Rowley *et al.*, Phys. Lett. B **373**, 23 (1996).
[8] I. I. Gontchar, D. J. Hinde, M. Dasgupta, and J. O. Newton, Nucl. Phys. A **722**, 479c (2003).
[9] K. Hagino, T. Takehi, A. B. Balantekin, and N. Takigawa, Phys. Rev. C **71**, 044612 (2005).
[10] K. Washiyama, K. Hagino, and M. Dasgupta, Phys. Rev. C **73**, 034607 (2006).
[11] L. R. Gasques *et al.*, Phys. Rev. C **76**, 024612 (2007).
[12] O. A. Capurro, J. O. Fernandez Niello, A. J. Pacheco, and P. R. S. Gomes, Phys. Rev. C **75**, 047601 (2007).
[13] M. Evers, M. Dasgupta, D. J. Hinde, L. R. Gasques, M. L. Brown, R. Rafiei, and R. G. Thomas, Phys. Rev. C **78**, 034614 (2008).
[14] K. Zerva *et al.*, Phys. Rev. C **80**, 017601 (2009).
[15] A. Pakou *et al.*, Phys. Lett. B **556**, 21 (2003).
[16] A. Pakou *et al.*, Phys. Rev. C **69**, 054602 (2004).
[17] I. J. Thompson, Comput. Phys. Rep. **7**, 167 (1988).
[18] C. J. Lin *et al.*, Nucl. Phys. A **787**, 281c (2007).
[19] D. S. Monteiro *et al.*, Phys. Rev. C **79**, 014601 (2009).
[20] J. Lubian, T. Correa, P. R. S. Gomes, and L. F. Canto, Phys. Rev. C **78**, 064615 (2008).
[21] S. Mukherjee, B. K. Nayak, D. S. Monteiro, J. Lubian, P. R. S. Gomes, S. Appannababu, and R. K. Choudhury, Phys. Rev. C **80**, 014607 (2009).
[22] D. R. Otomar *et al.*, Phys. Rev. C **80**, 034614 (2009).
[23] M. A. Nagarajan, C. C. Mahaux, and G. R. Satchler, Phys. Rev. Lett. **54**, 1136 (1985).
[24] A. Pakou *et al.*, Eur. Phys. J. A **39**, 187 (2009).
[25] N. Keeley, S. J. Bennett, N. M. Clarke, B. R. Fulton, G. Tungate, P. V. Drumm, M. A. Nagarajan, and J. S. Lilley, Nucl. Phys. A **571**, 326 (1994).
[26] J. M. Figueira *et al.*, Phys. Rev. C **81**, 024613 (2010).
[27] A. Pakou *et al.*, Phys. Lett. B **633**, 691 (2006).
[28] A. Pakou *et al.*, Phys. Rev. Lett. **90**, 202701 (2003).
[29] A. Pakou *et al.*, Phys. Rev. C **76**, 054601 (2007).